

Immobilization of urease onto cellulose spheres for the selective removal of urea

Miaomiao Lv · Xiaofei Ma  · Debbie P. Anderson · Peter R. Chang

Received: 27 May 2017 / Accepted: 17 November 2017 / Published online: 24 November 2017
© Springer Science+Business Media B.V., part of Springer Nature 2017

Abstract Cellulose spheres were selected as an economical and biodegradable carrier for urease immobilization. The high crystallinity cellulose spheres (Ces) were crosslinked using citric acid and then oxidized using sodium periodate to produce aldehyde groups on the Ces surface that would bind covalently with the amino groups of urease through a Schiff base reaction. Ces, the obtained dialdehyde cellulose spheres (DACes) and cellulose spheres immobilized by urease (UrCes) were characterized by FTIR, XRD, SEM and TG. The results demonstrated the successful modification of Ces and immobilization of urease, along with the retention of the

original spherical morphology and improved thermal stability. As an adsorbent, UrCes had both a greater adsorption capacity for urea and a greater specific selective adsorption than DACes. Urease was respectively immobilized on DACes with 19, 31 and 45% aldehyde contents to obtain UrCes1, UrCes2 and UrCes3. The maximum removal capacities of UrCes1, UrCes2, and UrCes3 for urea were 243.3, 276.2, and 187.6 mg g⁻¹, while only 10.71, 15.08 and 20.50 mg g⁻¹ L-phenylalanine were adsorbed, respectively.

Keywords Cellulose · Aldehyde group · Immobilization · Urease · Selective adsorption

M. Lv · X. Ma (✉)
Chemistry Department, School of Science, Tianjin University, Tianjin 30054, China
e-mail: maxiaofei@tju.edu.cn

X. Ma
National Demonstration Center for Experimental Chemistry & Chemical Engineering Education, Tianjin University, Tianjin 300354, China

D. P. Anderson · P. R. Chang (✉)
Bioproducts and Bioprocesses National Science Program, Agriculture and Agri-Food Canada, 107 Science Place, Saskatoon, SK S7N 0X2, Canada
e-mail: peter.chang@agr.gc.ca

P. R. Chang
Department of Chemical and Biological Engineering, University of Saskatchewan, Saskatoon, SK S7N 5A9, Canada

Introduction

Cellulose, one of the most abundant and widely distributed natural polymers, is composed of β -1,4 linked D-glucose units with many hydroxyl groups (Ma et al. 2016), and it accounts for more than 50% of the carbon content of plants. Many attractive properties, such as biodegradability, biocompatibility, non-toxicity, and low cost (Mahmoudian et al. 2012), make cellulose a hopeful renewable resource for meeting the demands of reducing the environmental footprint (Qiao et al. 2016). Studies on cellulose have been extensively carried out, including its structural

analysis (Leppänen et al. 2009), chemical modification (Kang et al. 2015), and regenerated cellulose materials (Wang et al. 2016). Of particular interest is chemical modification to improve original properties or to introduce new chemical and physical functionalities to cellulose. Based on this, cellulose could act as adsorbents or carrier materials in various fields. Oxidization of cellulose with an $\text{H}_3\text{PO}_4\text{--NaNO}_2$ mixture was used to increase the content of carboxylic groups for use as an adsorbent of crystal violet and auramine-O (Martins et al. 2017). Tao et al. (2017) prepared a hybrid cellulose-based adsorbent (HM-cotton) containing a dot-plane composite adsorption system for removal of dyes and metal ions from aqueous media. Wang et al. (2017) selected carboxylated cellulose nanocrystals (CCNs) as novel support materials for molecularly imprinted polymers in preparation of magnetic CCNs for the separation and purification of six fluoroquinolones (FQs) from egg samples. The diverse chemical modifications provide cellulose with new and specific properties, to a large extent promoting the development of cellulose science and application.

The enzyme urease catalyzes the hydrolysis of urea to produce ammonia and carbon dioxide. Because the enzyme does not take part in the chemical reaction, its overall structure and catalytic activity are preserved; however urease requires nickel to be active and it binds very specifically and tightly to the metal ions (Balasubramanian and Ponnuraj 2010). When compared to its free form, immobilized urease generally has longer shelf-life, easier separation from the reaction system, and can be used repeatedly. Various methods of enzyme immobilization have been developed, primarily including adsorption, entrapment, and covalent bonding. Urease has been immobilized onto a polypyrrole film by physical adsorption for use as a biological sensing element (Prissanaroon-Ouajai et al. 2015). The urease was covalently immobilized on to an electrode made of hyperbranched polyester functionalized gold nanoparticles (Tiwari et al. 2009). There are also some novel methods of urease immobilization that are attracting growing attention. Guedidi et al. (2010) used a layer-by-layer self-assembly technique to immobilize trypsin and urease on polyacrylonitrile based membranes. Pogorilyi et al. (2016) and Sahoo et al. (2011) prepared modified magnetite nanoparticles to immobilize urease either by adsorption or surface grafting. Generally, the materials used

for the enzyme immobilization can be divided into organic and inorganic origin. Organic materials are suitable for both physical or covalent immobilization since they are easily chemically modified to match conditions for a given enzyme and its application (Jesionowski et al. 2014). There are mainly two categories including biopolymers, such as chitosan (Krishna et al. 2011), chitin (Pham et al. 2017), alginate (Danial et al. 2015), gelatin (Liang et al. 2005) and starch (Luo and Fu 2010) that have been used as a matrix for immobilization of urease. The other is synthetic compounds such as polypropylene, epoxy resins, polystyrene, ion exchanger (Barbosa et al. 2015; Fernandez-Lafuente 2009) and carbon nanotube (Guzik et al. 2014). The most common inorganic carriers are hydroxyapatite, titania and silicas, which can maintain native structure of the enzyme with catalytic site in an active conformation (Cantone et al. 2013; Jesionowski et al. 2014). With the development of immobilization methods, applications for immobilized urease have increased in many fields including use in the food industry for the removal of urea from beverages and food, for the reduction of urea content in agricultural effluent, and for blood detoxification by artificial kidneys (Monier and El-Sokkary 2012). Consequently, the idea of using immobilized urease for the highly selective removal of the body's excess urea should be explored further.

The use of cellulose for enzyme immobilization has gained a wide range of interest (Nikolic et al. 2017; Soltani Firooz et al. 2017; Talingtaisong et al. 2017). Cellulose is hydrophilic but insoluble in water due to its hydroxyl groups, which are favorable supports for enzyme immobilization (Klemm et al. 2005), and the hydrogen bonds between cellulose molecules lead to its relatively stability. Many different chemical treatments have been used to modify cellulose, activate it, and broaden its application. Among these treatments, periodate oxidation is an important, highly specific and selective oxidation reaction, which breaks the C2–C3 bond of the glucopyranoside ring to form two aldehyde groups (Cheng et al. 2014; Sun et al. 2015). Enzymes could be immobilized on the treated cellulose via Schiff base reactions with the aldehyde groups. Based on this method, a variety of cellulose materials have been successfully modified and applied to enzyme immobilization, such as viscose fibers immobilized with trypsin (Nikolic et al. 2014), pulp fiber immobilized with pectinase (Wu et al. 2013), and

cotton fibers immobilized with urease (Monier and El-Sokkary 2012). Almost all of them focused on determining the optimal immobilization conditions, and seldom studied the adsorption performance of the immobilized enzymes to extend their practical worth. The modification and application of spherical powdered cellulose in urease immobilization has rarely been carried out.

In this work, novel cellulose spheres (Ces) were crosslinked with citric acid, and then oxidized by NaIO₄ to introduce dialdehyde groups. Urease was immobilized onto the dialdehyde cellulose (DACes) through a Schiff base reaction between the amine groups of the enzyme and the aldehyde groups of the modified cellulose spheres. In order to gain biologically active cellulose as an effective enzyme preparation adsorbent, we have investigated the adsorption behavior both of urea and amino acids, which showed ideal specific selectivity for the adsorption of urea. Cellulose chemical surface modification not only provides a new possibility for removing urea nitrogen specifically by oral administration, which is of great significance to future clinical treatment applications, but also expands the scope for cellulose to be used as a carrier material.

Materials and methods

Materials

Cellulose spheres (Ces) were procured from InnoTech Alberta (Edmonton, Alberta, Canada). Urease (enzyme activity ≥ 45 units/mg dry weight) from jack bean was purchased from Aladdin Industrial Corporation (Shanghai, China). L-phenylalanine, 99% purity, was provided by J&K Scientific (Beijing, China). All other reagents used were commercially available and of analytical grade.

Preparation of citric acid crosslinked Ces (CACes)

Citric acid (1 g) was dissolved in ethanol to form a solution into which the Ces (5 g) were immersed and uniformly dispersed. The mixture was dried at 60 °C to remove ethanol and then allowed to react in a forced air oven for 2 h at 110 °C (Ma et al. 2017). After

cooling, the dry mixture was washed several times with distilled water to remove superfluous citric acid, and then air-dried at room temperature to obtain CACes.

Periodate oxidation of CACes (DACes)

The pH of 150 mL distilled water was adjusted to 3.0 with 0.1 M sulfuric acid solution. CACes and sodium periodate were quickly added to the solution. The molar ratio between sodium periodate and CACes was 2:1 (Ma et al. 2017). The reaction was processed in the dark at 35 °C for 1–3 h with constant mechanical stirring and then cooled to room temperature. 5 mL Ethylene glycol was added to deplete the unreacted sodium periodate. The mixture was then filtered and washed several times with distilled water until the pH was 7.0, followed by washing with anhydrous ethanol to remove the water. The powders were dried at 50 °C and DACes with different aldehyde contents were obtained.

Immobilization of urease on DACes

60 mg urease was dispersed in 5 mL phosphate buffer solution (pH 7.0) and 1.0 g DACes was added to the enzyme solution. The reaction was processed at 30 °C for 4 h with constant stirring. The suspension was then filtered to remove unbound enzyme and washed with distilled water. The resultant immobilized urease on DACes (UrCes) was stored in refrigerator at 4 °C.

Determination of aldehyde content

The aldehyde content of DACes was determined according to the method of Yu et al. (2010) with some modification. Hydroxylamine hydrochloride (0.43 g) was dissolved in 30 mL distilled water. Subsequently, DACes (0.1 g) were added and the pH of the solution was adjusted to 4.5 with 0.1 M NaOH solution. The conversion of aldehydes into oximes continued at room temperature for 24 h. The aldehyde content was calculated using Eq. (1) with 0.1 g CACes used as the control.

$$(\text{CHO}\%) = \frac{(V_{\text{sample}} - V_{\text{control}}) \times C \times 162}{0.1 \times 1000} \times 100\% \quad (1)$$

V_{sample} (mL) is the consumption of NaOH (0.1 M) by DACes, V_{control} (mL) is the consumption of NaOH (0.1 M) by CACes, C (mol/L) is the concentration of NaOH (0.1 M), and 162 is the molar mass of glucose units (g/mol).

DACes with different aldehyde contents were obtained, which were labeled as DACe1, DACe2 and DACe3. The calculated aldehyde contents of DACe1, DACe2, and DACe3 were 19, 31, and 45%, respectively. The corresponding DACe1, DACe2 and DACe3 with immobilized urease were labeled as UrCes1, UrCes2, and UrCes3, respectively.

Characterization

FTIR analysis of Ces, CACes, DACes, and UrCes was performed at 2 cm^{-1} resolution on a Bio-Rad FTS3000 IR Spectrum Scanner. Pellets were prepared from the powder samples using KBr.

X-ray diffraction patterns of Ces, CACes, DACes and UrCes powders were recorded in the reflection mode over the angular range of $10\text{--}40^\circ$ (2θ) at ambient temperature on a Rigaku D/MAX-2500 operated at a $\text{CuK}\alpha$ wavelength of 1.542 \AA .

Thermogravimetric analysis (TG) of Ces, CACes, DACes and UrCes powders were done on a ZTY-ZP thermal analyzer. Samples were heated from room temperature to $500\text{ }^\circ\text{C}$ at a heating rate of $10\text{ }^\circ\text{C}/\text{min}$ in a nitrogen atmosphere.

The external surfaces of CACes, DACes, and UrCes powders were viewed using a Hitachi S-4800 scanning electron microscope. The powders were dispersed into ethanol using ultrasonication for 5 min. Drops of the suspension were drawn onto a glass flake, dried to remove ethanol, and coated under vacuum with gold. In order to examine the immobilized urease containing nickel, SEM mapping of the distribution of carbon, nitrogen, and nickel on the UrCes surfaces was measured as well.

Adsorption experiments

CACes, DACes, or UrCes (10 mg) were added into 20 mL glass bottles containing 10 mL 100 mg L^{-1} urea solution. The glass bottles were placed on a water bath shaker at $30\text{ }^\circ\text{C}$ (100 rpm) to reach adsorption equilibrium. Residual urea concentration was determined according to the method GB/T 18204. 29–2000

(China) using diacetylmonoxime-antipyrine. UV–vis spectrometry (UV-1800PC spectrophotometer, Mapada Instruments, Shanghai, China) at 460 nm was used to determine the urea adsorption capacity of UrCes (Liu et al. 2014). The initial concentration of urea was changed from 50 to 400 mg L^{-1} to study the adsorption isotherm. The experiments were repeated three times. After the removal process, the UrCes adsorbent was separated by centrifugation from the residual urea solution and washed with distilled water to remove the remaining external urea. The reusability of UrCes was then investigated.

The selective adsorption performance of UrCes was studied under the same conditions by adding 5.0 g L^{-1} L-phenylalanine to the 100 mg L^{-1} urea solution. Standard curves were used to measure the concentration of L-phenylalanine by UV–vis spectrometry at 257 nm.

Results and discussion

Characterization of Ces particles and derivatives

FTIR

Figure 1 shows the FTIR spectra of Ces, CACes, DACes, and UrCes2. The broad band at 3386 cm^{-1} was attributed to --OH stretching of cellulose (Liu et al. 2014). The peak at 2900 cm^{-1} was formed by C--H stretching of --CH_2 group (Nikolic et al. 2014), and the peaks near 1060 cm^{-1} were ascribed to C--O bond

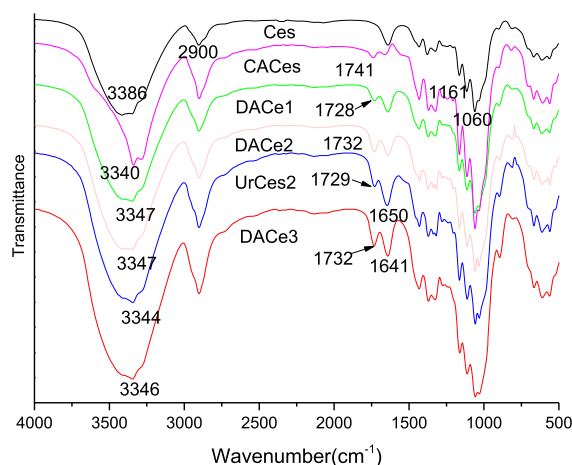


Fig. 1 FTIR spectra of Ces, CACes, DACes, and UrCes

stretching of $-C-O-C$ groups in the anhydroglucose ring of cellulose (Ma et al. 2016). A new peak at 1741 cm^{-1} that appeared in the spectra of CACes resulted from ester bonds produced by crosslinking. After oxidation with NaIO_4 , the characteristic absorption peak in DACes at 1728 cm^{-1} indicated the formation of dialdehyde groups (Jiang et al. 2016), which overlapped with the ester bond peaks of DACe2. Due to the transformation of $-C-OH$ groups into aldehyde groups, the relative intensity between $-C-O$ bond stretching of the anhydroglucose ring and the $-CH_2-$ group at 2935 cm^{-1} decreased gradually as the dialdehyde group content increased in DACe1, DACe2, and DACe3 (Ma et al. 2017). After coupling with urease, the characteristic absorption band in UrCes2 appeared at 1650 cm^{-1} and was attributed to the $C=N$ bond of the Schiff base; however, the absorption band of absorbed water at 1641 cm^{-1} may overlap with this band (Wu et al. 2013). In addition, the peak intensity of the carbonyl groups at 1729 cm^{-1} weakened because of the depletion of aldehyde groups due to the Schiff base reaction.

X-ray diffraction

The X-ray diffraction patterns of Ces and derivatives are exhibited in Fig. 2. Ces displayed the characteristic peaks of cellulose I including a strong peak (200) at a 2 theta value of 22.4° , two overlapped weaker peaks at 14.8° (1–10) and 16.4° (110), and a weak peak (004) at about 34.4° (Duchemin and Staiger

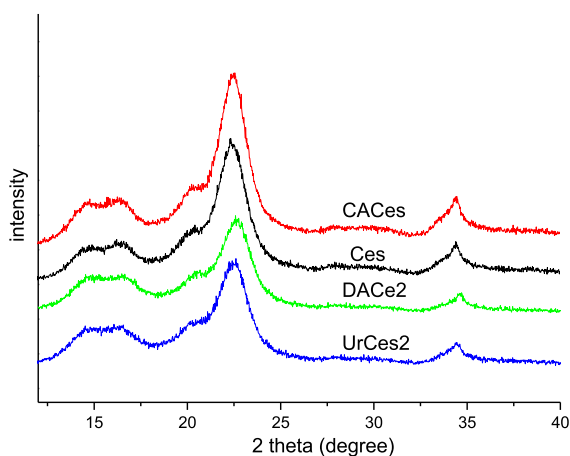


Fig. 2 X-ray diffraction patterns of Ces, CACes, DACe2, and UrCes2

2009). The different aldehyde contents led to small differences in the patterns of DACes and UrCes, represented in Fig. 2 by DACe2 and UrCes2. The patterns of Ces, CACes, and DACe2 were nearly identical, implying that the crystalline regions of native cellulose spheres were not destroyed by citric acid and NaIO_4 , and that the crosslinking reaction may protect the crystalline structure from being damaged. The crystalline regions of DACe2 were maintained after the Schiff base reaction with urea, which is reflected in the pattern of UrCes2. Modification of cellulose primarily occurred on the surface so that the native cellulose crystal structure was not disturbed (Spinella et al. 2016).

Thermogravimetric analysis

Thermal stability of Ces, CACes, DACe2, and UrCes2 was analyzed by thermogravimetric testing, the results of which are displayed in Fig. 3. A two-step degradation was observed in the curves with the first step at below 150°C attributed to loss of bound water, which provides a tool to determine water affinity (Spinella et al. 2016). The second step at about 300°C was caused by the decomposition of cellulose. The weight losses of Ces, CACes, and DACe2 at 150°C were very close, while the value for UrCes2 was larger. This trend demonstrated that dialdehyde cellulose immobilized with urease had a higher water affinity, which was beneficial for the adsorption of urea from aqueous solution.

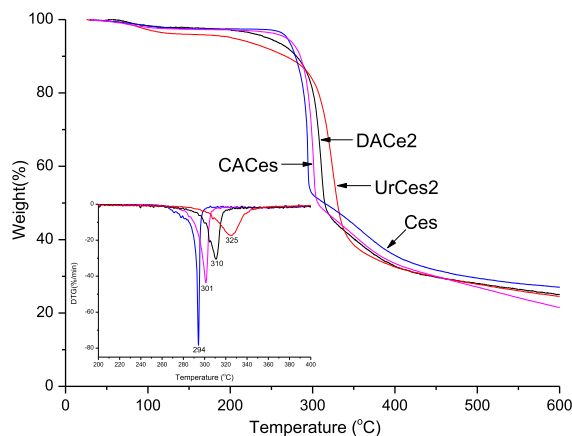


Fig. 3 TG and DTG curves of Ces, CACes, DACe2, and UrCes2

The differential thermogravimetric (DTG) curve shows the temperature at the maximum rate of degradation (T_{\max}). T_{\max} for Ces was 294 °C and 301 °C for CACes with a 41% weight loss. For DACe2 and UrCes2, T_{\max} occurred at 310 and 325 °C, respectively. Compared to Ces, crosslinking citric acid improved the T_{\max} for CACes slightly. Moreover, dialdehyde groups improved interaction with cellulose hydroxyl groups, contributing to a higher degradation temperature for DACes. Immobilization of an enzyme in a support usually restricts its ability to undergo intense conformational changes resulting in increased stability toward denaturation (Monier and El-Sokkary 2012).

Scanning electron microscopy

Figure 4 shows the morphology of the original and modified celluloses. Figure 4a shows the sphere

structure of Ces. The isolated particles were monodisperse with diameters in the range of 2–10 μm. Crosslinking with citric acid did not significantly change the morphology of CACes (Fig. 4b). Multiple carboxyl groups of the citric acid crosslinker reacted with the cellulose hydroxyl groups helping to preserve the spherical shape after the periodate oxidative cleavage of the C-2 and C-3 bonds of the anhydroglucose units (Ma et al. 2017). Accordingly, there is no obvious change in the surface of DACe2 particles (Fig. 4c). Compared to DACe2, the surface of UrCes2 (Fig. 4d) was slightly rougher because the urease modification occurred on the sphere surface.

SEM mapping images of UrCes2 are shown in Fig. 5. Because urease is an oligomeric enzyme containing nickel and nitrogen, these elements were introduced into UrCes via Schiff base reactions between the urease amino groups and the aldehyde groups of DACes. The distributions of carbon

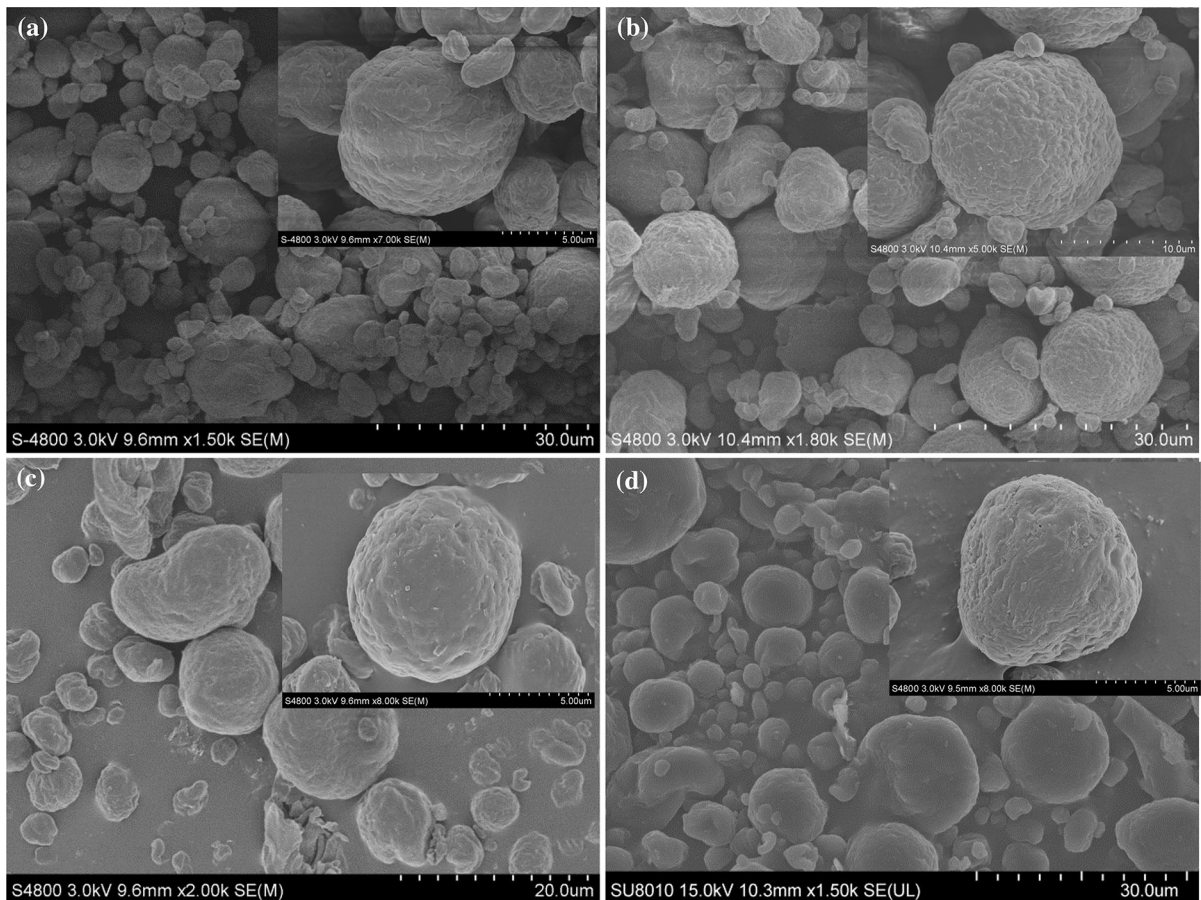


Fig. 4 SEM micrographs of Ces (a), CACes (b), DACe2 (c) and UrCes2 (d)

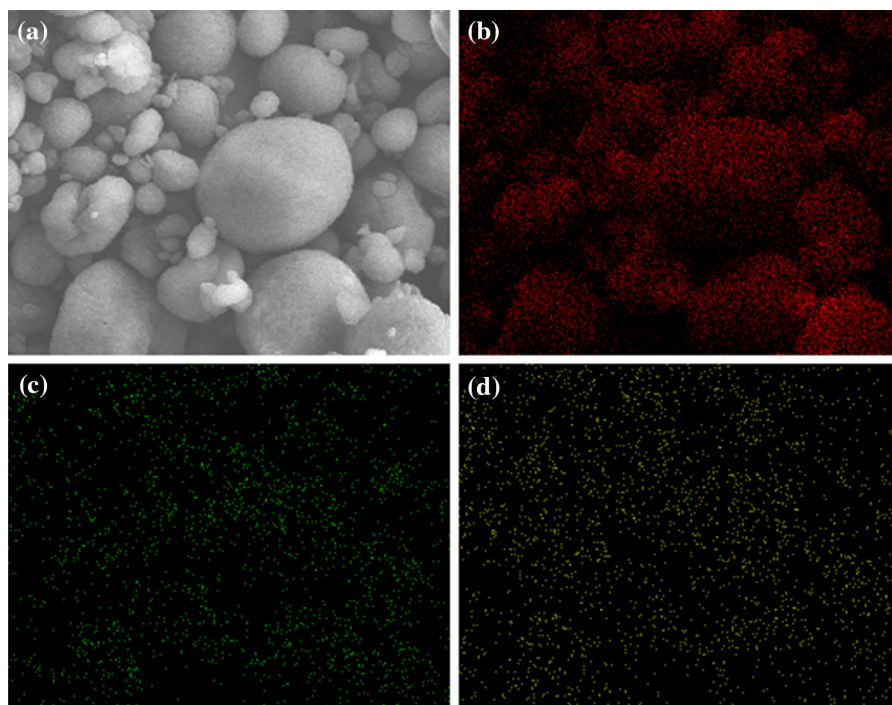


Fig. 5 SEM Mapping images of UrCes2 (a) and UrCes2 C (b), N (c), and Ni (d)

(Fig. 5b), nitrogen (Fig. 5c), and nickel (Fig. 5d) on the surface of the UrCes2 sphere are reflected in the photographs. As can be seen, nickel and nitrogen were evenly distributed, which demonstrated that the urease had been uniformly immobilized on the DACes surface.

Batch adsorption kinetic and isotherm modeling

The effect of contact time on the removal of urea by DACes and UrCes is shown in Fig. 6a, b. The pseudo-first-order kinetic model and pseudo-second-order kinetic model, expressed in Eq. (2) and Eq. (3), respectively, was applied to investigate the removal kinetics:

$$\log(q_e - q_t) = \log q_e - k_1 t \quad (2)$$

$$\frac{t}{q_t} = \frac{1}{k_2 q_e^2} + \frac{t}{q_e} \quad (3)$$

where q_t (mg g^{-1}) is the amount of urea removed at time t (min); k_1 (min^{-1}) and k_2 ($\text{mg g}^{-1} \text{min}^{-1}$) are the rate constant of pseudo-first-order model and pseudo-second-order model, respectively; and q_e (mg g^{-1}) is

the amount of urea removed at equilibrium. The parameters are calculated from a linear plot of t/q_t against t .

The kinetic constants, R^2 , SSE, and the urea removal capacities of the kinetic models were calculated from experimental data and are listed in Fig. 6a, b. According to SSE, the removal behavior of DACes fitted pseudo-first-order model better than pseudo-second-order model, while the removal behavior of UrCes fitted the pseudo-second-order model better. But the values of R^2 confirmed a good agreement for the removal processes of both DACes and UrCes with the pseudo-second-order model.

The q_e values from the pseudo-second-order model indicated UrCes2 exhibited better removal of urea (93.90 mg g^{-1}) than both UrCes1 (83.82 mg g^{-1}) and UrCes3 (77.64 mg g^{-1}). The q_e values of DACe1, DACe2 and DACe3 were 18.18, 22.47 and 22.72 mg g^{-1} , respectively. In addition, Ces and CACes adsorbed 10.96 and 10.23 mg g^{-1} of urea, respectively. UrCes were treated at 65°C for 2 h to make the enzyme on UrCes inactivated. The inactivated-UrCes1, UrCes2 and UrCes3 only adsorbed 6.16 , 5.31 and 8.24 mg g^{-1} of urea, respectively. Suppose that urea was only absorbed by residual

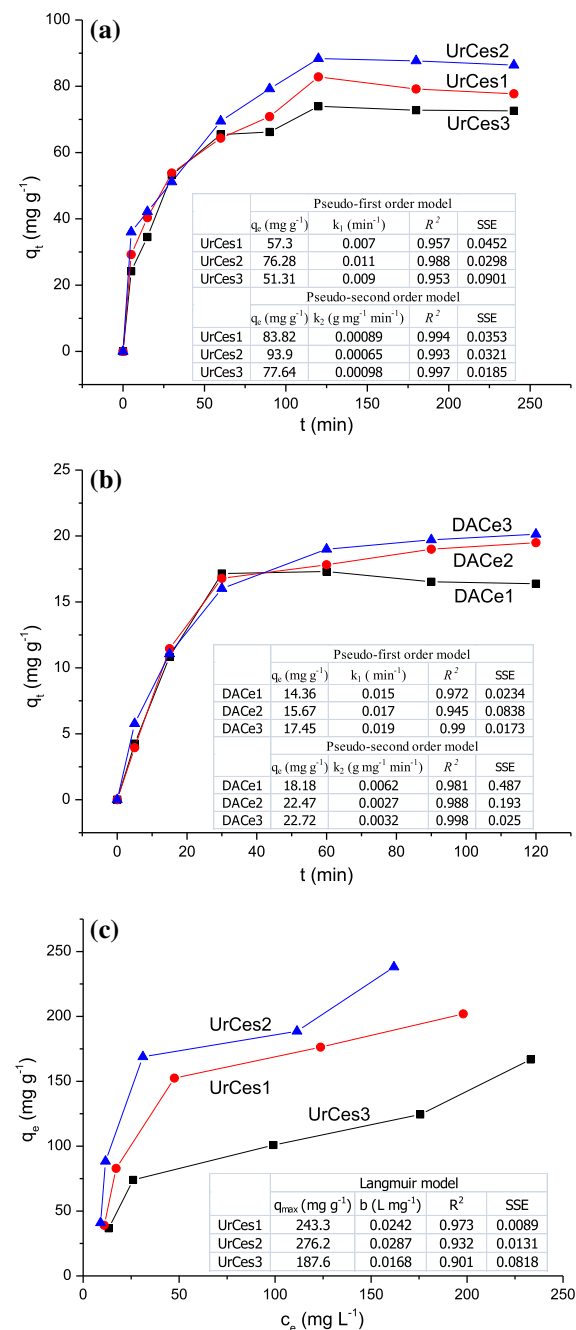


Fig. 6 Effect of contact time on adsorption of urea by UrCes (a) and DACes (b); inset is the pseudo-first-order model and pseudo-second-order model data for batch adsorption of urea by UrCes (a) and DACes (b), initial concentration: urea 100 mg L⁻¹, adsorbent 1.0 g L⁻¹. Adsorption isotherms (c) of urea by UrCes at 30 °C; inset is the Langmuir model data for adsorption of urea by UrCes (c), adsorbent 1.0 g L⁻¹

aldehyde group without the subsequent decomposition by the immobilized urease, percentage attributed to adsorption versus removal was 8.03, 6.39 and 12.54% for UrCes1, UrCes2, and UrCes3, respectively.

The hydroxyl groups of Ces and CACes could form the hydrogen bonding interaction with urea. The dialdehyde groups of DACes could produce the stronger interaction (the covalent Schiff base structure) with urea. DACe3 adsorbed more urea than other two because of more aldehyde group contents. The immobilized urease could decompose urea to CO₂ and ammonia. The removal of urea was the adsorption process for Ces, CACes and DACe, while that for UrCes involved both the adsorption and decomposition of urea. The inactivated-UrCes only adsorbed urea rather than hydrolyzed urea. The differences of the removal values (77.66, 88.59 and 69.40 mg g⁻¹) between the inactivated-UrCes and UrCes were related to the urease catalysis, which were used to estimate the urease loading or the catalytic activity for the hydrolysis of urea. Obviously, UrCes2 exhibited the better catalytic activity (88.59 mg g⁻¹), while UrCes3 had the lowest catalytic activity (69.40 mg g⁻¹). The greater number of aldehyde groups in DACe2 than in DACe1 provide increased chances for aldehyde and amino groups to come in contact and interact. Also, steric hindrance of DACe2 was lower than DACe3. These factors led to more urease being immobilized on DACe2, and hence, UrCes2 had a better urea removal capacity. Suppose that enzyme activity of urease remained unchanged before and after the immobilization, the amounts of urease immobilized on DACe supports were calculated to be approximately 2.85, 3.25 and 2.54% for UrCes1, UrCes2 and UrCes3, respectively.

The removal isotherm of urea by UrCes is displayed in Fig. 6c. The linear form of the Langmuir isotherm equation is as follows:

$$\frac{C_e}{q_e} = \frac{C_e}{q_{max}} + \frac{1}{bq_{max}} \quad (4)$$

where q_e (mg g⁻¹) is the amount of urea removed at equilibrium; q_{max} (mg g⁻¹) represents the maximum removal capacity of adsorbents; C_e (mg L⁻¹) is the equilibrium concentration of the urea solution; and b (L mg⁻¹) is the equilibrium constant of Langmuir adsorption. The values of b and q_{max} were calculated from the linear plot of C_e/q_e versus C_e .

The values of R^2 showed that the removal of urea for UrCes didn't fit much with the Langmuir model. Since many adsorbents were estimated for the urea removal capability in the Langmuir model, here the Langmuir model was still applied to UrCes to compare with the q_{\max} values from the references. In the Langmuir isotherm model, b is related to the bonding energy coefficient as well as a relevant indicator of the adsorption capacity. The value of b is larger for UrCes2 (0.0287 L mg^{-1}) than for both UrCes1 (0.0242 L mg^{-1}) and UrCes3 (0.0168 L mg^{-1}), implying that the urea removal capacity of UrCes2 is higher than that of UrCes1 and UrCes3, which is consistent with the measured values of q_{\max} . The maximum removal capacities for urea of UrCes2, UrCes1, and UrCes3 were 276.2 , 243.3 , and 187.6 mg g^{-1} , respectively, which were higher than those of other polysaccharide adsorbents such as porous starch xanthate and porous starch citrate (109.1 and 57.6 mg g^{-1}) (Ma et al. 2015), carboxymethyl sago starch-acid hydrogel (109.9 mg g^{-1}) (Basri et al. 2016), and magnetic chitosan microbeads (128.5 mg g^{-1}) (Oladipo and Gazi 2016).

Reusability of UrCes

Removal cycles of urea for UrCes1, UrCes2, and UrCes3 were also evaluated in Fig. 7. The removal efficiency (%) is the ratio of the mass of removal urea at any time compared to that of the first measurement. After five cycles, the removal efficiencies of urea for UrCes1, UrCes2, and UrCes3 were 92.27, 90.05 and 78.64%, respectively. The removal efficiency

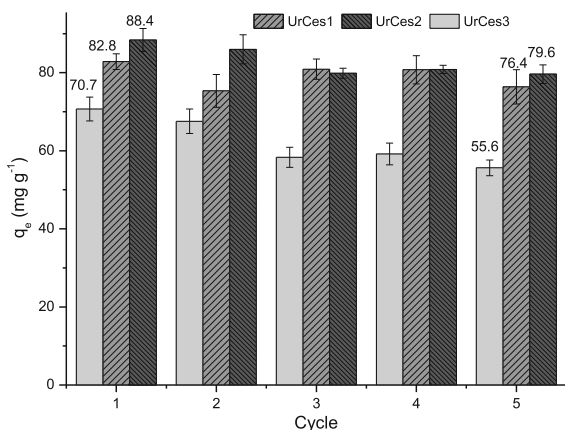


Fig. 7 Adsorption cycles of UrCes1, UrCes2 and UrCes3

decreased with time due to some loss of the adsorbent during washing. The removal capacity was still 90% for UrCes1 and UrCes2 after the fifth measurement, which embodied good reusability for the removal of urea.

Selective adsorption of UrCes

L-phenylalanine is an essential amino acid that cannot be synthesized by the human body and is used as a component of nutritional enhancers, amino acid infusions, and amino acid compound preparations. In this experiment, L-phenylalanine was used to study selective adsorption by UrCes. Results are shown in Fig. 8. Using a single solution of L-phenylalanine, the adsorption capacities of DACe1, DACe2, and DACe3 were 77.71 , 82.71 , and 88.31 mg g^{-1} , respectively, and only 11.06 , 17.96 , and 20.93 mg g^{-1} for UrCes1,

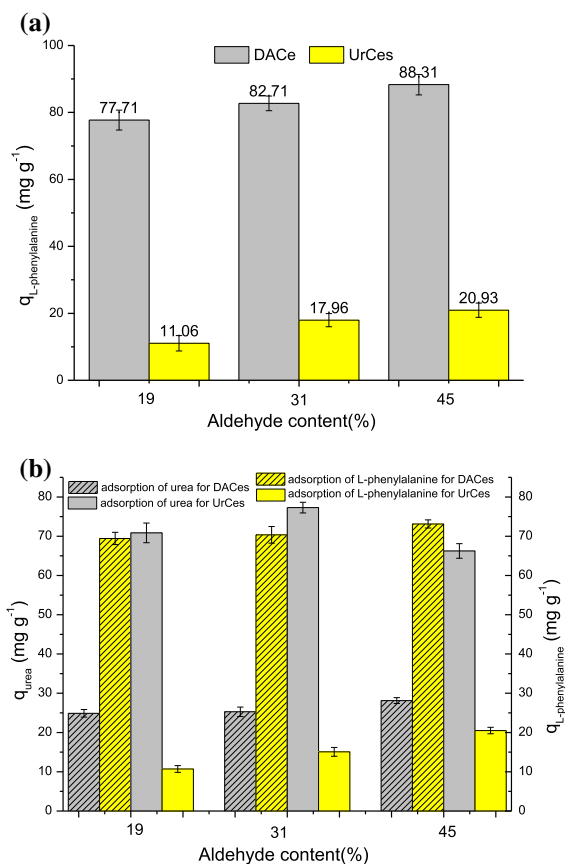


Fig. 8 Selective adsorption of urea and L-phenylalanine by DACes and UrCes in L-phenylalanine single solution (a) and in mixture (b). Initial concentration: urea 100 mg L^{-1} ; L-phenylalanine 5.0 g L^{-1}

UrCes2, and UrCes3, respectively (Fig. 8a). The numerous aldehyde groups on DACes promote its reaction with amino acids.

Using a mixture of urea and L-phenylalanine, selective adsorption was more evident. As can be seen in Fig. 8b, the amount of urea removal from the mixed solution by UrCes1, UrCes 2, and UrCes3 was 70.85, 77.29 and 66.25 mg g⁻¹, respectively, while only 10.71, 15.08, and 20.50 mg g⁻¹ of L-phenylalanine were adsorbed, respectively. By contrast, the adsorption capacity of DACe1, DACe2, and DACe3 for L-phenylalanine was 69.43, 70.36 and 73.13 mg g⁻¹, respectively, and only 24.89, 25.28 and 28.13 mg g⁻¹ adsorption capacity for urea. Compared to DACes, UrCes selectively remove the majority of urea but only a very small amount of amino acid. All in all, the adsorption capacity for urea and the selective adsorption of urea has been greatly improved through immobilization.

Conclusion

DACes were successfully prepared by crosslinking with citric acid followed by oxidization with NaIO₄. Urease was immobilized on a modified cellulose sphere adsorbent, which exhibited superior selective adsorption and removal of urea from aqueous solutions. The removal of urea from aqueous solution was complete in a short time with a favorable adsorption capacity and high removal efficiency. This process fit both the pseudo-second-order kinetic model and the Langmuir isotherm model. The percentage attributed to adsorption versus removal was 8.03, 6.39 and 12.54% for UrCes1, UrCes2, and UrCes3, respectively. The maximum removal capacity of UrCes2 for urea was 276.24 mg g⁻¹. Meanwhile, amino acids in the aqueous solution were well retained. This immobilization remarkably improved the removal capacity for urea, reusability, and selective removal, which is of realistic significance in the medical applications or agricultural wastewater treatment. The study of previous surface modification demonstrated that as a carrier material or an adsorbent, cellulose can be exploited further for more practical applications.

Acknowledgments This research was supported by the National Nature Science Foundation of China (51462009 and 51662011).

References

- Balasubramanian A, Ponnuraj K (2010) Crystal structure of the first plant urease from jack bean: 83 years of journey from its first crystal to molecular structure. *J Mol Biol* 400:274–283
- Barbosa O, Ortiz C, Berenguer-Murcia A, Torres R, Rodrigues RC, Fernandez-Lafuente R (2015) Strategies for the one-step immobilization-purification of enzymes as industrial biocatalysts. *Biotechnol Adv* 33:435–456
- Basri SN, Zainuddin N, Hashim K, Yusof NA (2016) Preparation and characterization of irradiated carboxymethyl sago starch-acid hydrogel and its application as metal scavenger in aqueous solution. *Carbohydr Polym* 138:34–40
- Cantone S, Ferrario V, Corici L, Ebert C, Fattor D, Spizzo P, Gardossi L (2013) Efficient immobilisation of industrial biocatalysts: criteria and constraints for the selection of organic polymeric carriers and immobilisation methods. *Chem Soc Rev* 42:6262–6276
- Cheng Y, Lu J, Liu S, Zhao P, Lu G, Chen J (2014) The preparation, characterization and evaluation of regenerated cellulose/collagen composite hydrogel films. *Carbohydr Polym* 107:57–64
- Danial EN, Hamza AH, Mahmoud RH (2015) Characteristics of Immobilized Urease on Grafted Alginate Bead Systems. *Braz Arch Biol Technol* 58:147–153
- Duchemin B, Staiger MP (2009) Treatment of Harakeke fiber for biocomposites. *J Appl Polym Sci* 112:2710–2715
- Fernandez-Lafuente R (2009) Stabilization of multimeric enzymes: strategies to prevent subunit dissociation. *Enzyme Microb Technol* 45:405–418
- Guedidi S et al (2010) Effect of enzyme location on activity and stability of trypsin and urease immobilized on porous membranes by using layer-by-layer self-assembly of polyelectrolyte. *J Membr Sci* 365:59–67
- Guzik U, Hupert-Kocurek K, Wojcieszynska D (2014) Immobilization as a strategy for improving enzyme properties-application to oxidoreductases. *Molecules* 19:8995–9018
- Jesionowski T, Zdarta J, Krajewska B (2014) Enzyme immobilization by adsorption: a review. *Adsorption* 20:801–821
- Jiang X, Yang Z, Peng Y, Han B, Li Z, Li X, Liu W (2016) Preparation, characterization and feasibility study of dialdehyde carboxymethyl cellulose as a novel crosslinking reagent. *Carbohydr Polym* 137:632–641
- Kang H, Liu R, Huang Y (2015) Graft modification of cellulose: methods, properties and applications. *Polymer* 70:A1–A16
- Klemm D, Heublein B, Fink HP, Bohn A (2005) Cellulose: fascinating biopolymer and sustainable raw material. *Angew Chem Int Ed Engl* 44:3358–3393
- Krishna BL, Singh AN, Patra S, Dubey VK (2011) Purification, characterization and immobilization of urease from *Momordica charantia* seeds. *Process Biochem* 46:1486–1491
- Leppänen K, Andersson S, Torkkeli M, Knaapila M, Kotelnikova N, Serimaa R (2009) Structure of cellulose and microcrystalline cellulose from various wood species, cotton and flax studied by X-ray scattering. *Cellulose* 16:999–1015
- Liang ZP, Feng YQ, Liang ZY, Meng SX (2005) Adsorption of urea nitrogen onto chitosan coated dialdehyde cellulose

- under biocatalysis of immobilized urease: equilibrium and kinetic. *Biochem Eng J* 24:65–72
- Liu X, Chang PR, Zheng P, Anderson DP, Ma X (2014) Porous cellulose facilitated by ionic liquid [BMIM]Cl: fabrication, characterization, and modification. *Cellulose* 22:709–715
- Luo Z, Fu X (2010) Immobilization of urease on dialdehyde porous starch. *Starch—Stärke* 62:652–657
- Ma X, Liu X, Anderson DP, Chang PR (2015) Modification of porous starch for the adsorption of heavy metal ions from aqueous solution. *Food Chem* 181:133–139
- Ma X, Liu C, Anderson DP, Chang PR (2016) Porous cellulose spheres: preparation, modification and adsorption properties. *Chemosphere* 165:399–408
- Ma X, Lv M, Anderson DP, Chang PR (2017) Natural polysaccharide composites based on modified cellulose spheres and plasticized chitosan matrix. *Food Hydrocoll* 66:276–285
- Mahmoudian S, Wahit MU, Ismail AF, Yussuf AA (2012) Preparation of regenerated cellulose/montmorillonite nanocomposite films via ionic liquids. *Carbohydr Polym* 88:1251–1257
- Martins LR, Rodrigues JA, Adarme OF, Melo TM, Gurgel LV, Gil LF (2017) Optimization of cellulose and sugarcane bagasse oxidation: application for adsorptive removal of crystal violet and auramine-O from aqueous solution. *J Colloid Interface Sci* 494:223–241
- Monier M, El-Sokkary AM (2012) Modification and characterization of cellulosic cotton fibers for efficient immobilization of urease. *Int J Biol Macromol* 51:18–24
- Nikolic T, Milanovic J, Kramar A, Petronijevic Z, Milenkovic L, Kostic M (2014) Preparation of cellulosic fibers with biological activity by immobilization of trypsin on periodate oxidized viscose fibers. *Cellulose* 21:1369–1380
- Nikolic T, Korica M, Milanovic J, Kramar A, Petronijevic Z, Kostic M (2017) TEMPO-oxidized cotton as a substrate for trypsin immobilization: impact of functional groups on proteolytic activity and stability. *Cellulose* 24:1863–1875
- Oladipo AA, Gazi M (2016) Hydroxyl-enhanced magnetic chitosan microbeads for boron adsorption: parameter optimization and selectivity in saline water. *React Funct Polym* 109:23–32
- Pham ML et al (2017) Immobilization of beta-Galactosidases from *Lactobacillus* on Chitin using a Chitin-binding domain. *J Agric Food Chem* 65:2965–2976
- Pogorilyi RP, Melnyk IV, Zub YL, Seisenbaeva GA, Kessler VG (2016) Enzyme immobilization on a nano-adsorbent for improved stability against heavy metal poisoning. *Colloids Surf B Biointerfaces* 144:135–142
- Prissanaroon-Ouajai W, Sirivat A, Pigram PJ, Brack N (2015) Potentiometric urea biosensor based on a urease-immobilized polypyrrole. *Macromol Symp* 354:334–339
- Qiao C, Chen G, Zhang J, Yao J (2016) Structure and rheological properties of cellulose nanocrystals suspension. *Food Hydrocolloids* 55:19–25
- Sahoo B, Sahu SK, Pramanik P (2011) A novel method for the immobilization of urease on phosphonate grafted iron oxide nanoparticle. *J Mol Catal B Enzyme* 69:95–102
- Soltani Firooz N, Panahi R, Mokhtarani B, Yazdani F (2017) Direct introduction of amine groups into cellulosic paper for covalent immobilization of tyrosinase: support characterization and enzyme properties. *Cellulose* 24:1407–1416
- Spinella S et al (2016) Concurrent cellulose hydrolysis and esterification to prepare a surface-modified cellulose nanocrystal decorated with carboxylic acid moieties. *ACS Sustain Chem Eng* 4:1538–1550
- Sun B, Hou Q, Liu Z, Ni Y (2015) Sodium periodate oxidation of cellulose nanocrystal and its application as a paper wet strength additive. *Cellulose* 22:1135–1146
- Talingtaison S, Vongsetskul T, Panatdasirisuk W, Tangboriboonrat P (2017) Gauze-reinforced electrospun regenerated cellulose ultrafine fibers for immobilizing bromelain. *Cellulose* 24:2967–2975
- Tao J, Xiong J, Jiao C, Zhang D, Lin H, Chen Y (2017) Cellulose/polymer/silica composite cotton fiber based on a hyperbranch-mesostructure system as versatile adsorbent for water treatment. *Carbohydr Polym* 166:271–280
- Tiwari A, Aryal S, Pilla S, Gong S (2009) An amperometric urea biosensor based on covalently immobilized urease on an electrode made of hyperbranched polyester functionalized gold nanoparticles. *Talanta* 78:1401–1407
- Wang S, Lu A, Zhang L (2016) Recent advances in regenerated cellulose materials. *Prog Polym Sci* 53:169–206
- Wang YF, Wang YG, Ouyang XK, Yang LY (2017) Surface-imprinted magnetic carboxylated cellulose nanocrystals for the highly selective extraction of six fluoroquinolones from egg samples. *ACS Appl Mater Interfaces* 9:1759–1769
- Wu R, He BH, Zhao GL, Qian LY, Li XF (2013) Immobilization of pectinase on oxidized pulp fiber and its application in whitewater treatment. *Carbohydr Polym* 97:523–529
- Yu J, Chang PR, Ma X (2010) The preparation and properties of dialdehyde starch and thermoplastic dialdehyde starch. *Carbohydr Polym* 79:296–300